Neuro-Oncology Advances

8(1), vdag102, 2026 | https://doi.org/10.1093/noajnl/vdag102 | Advance Access publication April 13, 2026

Clofoctol as a novel senolytic drug eliminating therapy-induced senescent glioma cells

Yuxin Zhang, Zhixing Wang, Yue Wang, Enyan Li, Fan Wu, Lin Hou, Bin Yin, Boqin Qiang, Wei Han, and Xiaozhong Peng

All author affiliations are listed at the end of the article

Corresponding Authors: Xiaozhong Peng, State Key Laboratory of Common Mechanism Research for Major Diseases, Department of Biochemistry & Molecular Biology, Institute of Basic Medical Sciences & School of Basic Medicine, Chinese Academy of Medical Sciences & Peking Union Medical College, Beijing, No. 5 Dongdan Santiao, Dongcheng District, Beijing 100005, China (pengxiaozhong@pumc.edu.cn); Wei Han, State Key Laboratory of Common Mechanism Research for Major Diseases, Department of Biochemistry & Molecular Biology, Institute of Basic Medical Sciences & School of Basic Medicine, Chinese Academy of Medical Sciences & Peking Union Medical College, Beijing, No. 5 Dongdan Santiao, Dongcheng District, Beijing 100005, China (hanwei2012@ibms.pumc.edu.cn).

Abstract

Background. Glioblastoma is the most common malignant brain glioma, accounting for ~48% of malignant central nervous system tumors. Targeting glioma stem cells and senescent glioma cells represents promising therapeutic strategies. In our previous study, we identified the clofoctol as a candidate drug targeting glioma stem cells with good blood-brain barrier permeability and potent anti-glioblastoma efficacy. Comprehensively demonstrating the impact of clofoctol on glioblastoma might provide novel strategies for the treatment of glioblastoma.

Methods. By utilizing single-cell RNA sequencing of tumor tissue, we demonstrated the suppression effect of clofoctol on senescent glioma cell. Cellular RNA sequencing, molecular docking and CETSA were used to further confirm target of clofoctol. Ultimately, GL261 and orthotopic patient-derived xenograft animal models was performed to assess whether the senolytic effect of clofoctol could enhance TMZ therapy.

Results. Clofoctol treatment reduced the senescence level (SASPs, senescence-related genes, and the proportion of senescent cells) in GL261-derived tumor single-cell RNA sequencing. In vitro, clofoctol could target senescent glioma cells and induce cell death through apoptosis and ferroptosis. P53 was identified as the functional protein which elicited the effect of clofoctol. In vivo, clofoctol exhibited senolytic activity and synergized with TMZ, leading to extended survival in glioblastoma mouse model.

Conclusions. Our study demonstrated the clinical drug clofoctol could target chemotherapy-induced senescent glioma cells through P53 and trigger cell apoptotic and ferroptotic death. We further confirmed a synergistic effect between clofoctol and temozolomide which could be a novel therapeutic approach for glioblastoma therapy.

Key Points

- Clofoctol eliminates senescent glioma cells as a novel senolytic drug.
- P53 is an effective target of clofoctol in senescent glioma cells.
- Clofoctol and TMZ synergistically inhibit glioma tumor growth *in vivo and in vitro*.

Glioblastoma (GBM) is the most aggressive and lethal brain tumor in adults. The patients usually have a poor prognosis with the median survival less than 2 years. The standard clinical approach for GBM is maximal safe surgical resection followed by radiotherapy and temozolomide (TMZ) chemotherapy.[1] However, some patients initially benefit from TMZ, tumor relapse typically occurs rapidly and are often refractory to further treatment, primarily due to intrinsic or acquired chemoresistance mechanisms,[2,3] including O6-methylguanine-DNA methyltransferase (MGMT) expression in glioma cell, mismatch repair when DNA damage happened, the persistence of glioma stem cell in tumor[4] and the therapy-induced cellular senescence.[5]

Received August 27, 2025; accepted April 8, 2026.

Importance of the Study

Glioblastoma (GBM) remains incurable due to therapy-resistant cell populations, including senescent cells that promote recurrence. While senolytic strategies show promise, few cross the blood-brain barrier (BBB) or target glioma effectively. We demonstrate that clofoctol, a BBB-permeable drug, functions as a senolytic agent by eliminating therapy-induced senescent glioma cells through P53-mediated apoptosis and ferroptosis.

Using single-cell transcriptomics, orthotopic PDX models, and mechanistic studies, we prove that clofoctol depletes senescent cells, synergizes with temozolomide (TMZ), and significantly extends survival. Our work identifies clofoctol as a novel senolytic drug for glioma that targets senescence cells, offering a potential approach to overcome resistance. This dual-action, repurposed strategy addresses an urgent need for combinatorial therapies against recurrent GBM.

Cellular senescence is a permanent cell cycle arrest accompanied by secretion of senescence-associated secretory phenotype (SASP), morphological transformation, and elevated senescence-associated β-galactosidase (SA-β-Gal) activity.[6,7] However, the impact of senescent cancer cell for tumor progress is complicated. While senescence initially limits tumor cell proliferation and SASP components may promote immune-mediated clearance,[8,9] accumulating evidence suggests that sustained SASP signaling ultimately creates a tumor-promoting microenvironment through multiple mechanisms, including chronic inflammation, mitogenic stimulation, stemness maintenance, angiogenesis promotion, and immunosuppression.[7,10,11] In GBM, it has been proved that senescent cancer cells represent a pro-tumor function in vivo. Recent investigations using orthotopic patient-derived xenografts (PDX) and transgenic mouse models of GBM reveal that targeted clearance of senescent cells suppresses tumor proliferation and enhances overall survival.[5,12,13]These findings position senescent cells targeting as a promising therapeutic strategy for GBM, yet several critical questions remain unresolved: (1) Which senolytic agents show optimal efficacy for GBM treatment? (2) Could senotherapy be effectively combined with standard therapies like TMZ chemotherapy or radiotherapy?

Based on the huge financial and time burden to discovery new drug, for GBM therapy, we used unbiased drug screening on 1920 compounds from the MicroSource Spectrum Collection in previous work, and defined clofoctol (Clo) as a glioma stem cell targeted drug which represent robust anticancer effect in vivo and in vitro.[14] Clo is an antibacterial drug for Gram-positive bacteria, such as *Streptococcus, pyogenes* and *Streptococcus pneumoniae*, common pathogens of upper and lower respiratory tract infections.[15] Recently, it has also been investigated for its anti-tumor properties by activating unfolded protein response (UPR)[16] and anti-inflammatory function by decreasing the transcription of inflammatory markers like interleukin 6 (IL-6), tumor necrosis factor (TNF) α, interferon (IFN) β, IFNγ.[17] Evidences suggest that senescence SASPs evoke chronic inflammatory microenvironment to promote tumorigenesis[18] while cancer cell could acquire stem-cell features after senescence occur by senescence related genes Bmi-1, p16, p21, or p53,[19] which indicate overlapping signaling networks between stemness, inflammation and senescence in tumor.[20] These observations raise an important question: could Clo influence cellular senescence processes?

In this study, we determined Clo to be a senolytic drug in vitro and in vivo. Single-cell RNA sequencing analysis of Clo-treated GL261-derived tumors revealed a reduction in senescence features. We further validated Clo's senolytic activity using two distinct models of therapy-induced senescence (TIS) established by temozolomide and doxorubicin (DOX) treatment. Moreover, integrating RNA sequencing (RNA-seq), molecular docking, and cellular thermal shift assay analyses (CETSA) identified p53 as the primary molecular target of Clo in senescent glioma cells. Mechanistically, Clo binds to the asparagine-288 (Asn-288) residue of p53, concurrently activating both apoptotic and ferroptotic cell death pathways. Ultimately, we evaluated the combined therapeutic efficacy of TMZ and Clo in both PDX and GL261 orthotopic glioma models. Our results demonstrate a synergistic anti-tumor effect of this drug combination in GBM.

Methods

Cell Culture and Lentivirus

Murine GBM cell line GL261 and the patient-derived glioma cell line T3-5 were obtained from Beijing Tiantan Hospital. Human GBM cell lines LN229 and U87MG were purchased from American Type Culture Collection (ATCC). GL261 and LN229 were maintained in DMEM (Gibco) media with 10% FBS (Gibco), 1% 100×Antibiotic-Antimycotic (Gibco). T3-5 was cultured in neurobasal medium (Gibco) supplemented with 2% B-27 (Gibco), 1% 100× Antibiotic-Antimycotic (Gibco), 2 mmol/L l-glutamine (catalog SH30034.01, HyClone), 20 ng/mL basic fibroblast growth factor (bFGF; catalog 100-18B-50UG PeproTech), 20 ng/mL epidermal growth factor (EGF; catalog AF-100-15-100UG, PeproTech), 10 μg/mL heparin (Sigma-Aldrich). P53 knockdown LN229 (LN229-shP53) was generated by lentivirus transduction and 2 μg/mL puromycin was used to purify. The lentivirus is purchased from Genechem, shanghai. The clofoctol treatment concentration for GL261, LN229, and U87MG was 50 μM and for T3-5 was 20 μM expect otherwise stated.

Mouse Orthotopic Tumorigenesis

To establish traceable tumor models, we generated luciferase-expressing GL261 cells (GL261-luc) through lentiviral transduction. We orthotopically injected 5×10^5 GL261-luc cells into male C57BL/6J mice (5-6 weeks).

A midline scalp incision was made and a burr-hole was created 1.0 mm anterior to the bregma and 2.0 mm lateral to the midline using a high-powered drill. Then, cells were transplanted into the burr-hole to a depth of 3 mm using the injection needle of a Hamilton syringe (Hamilton-10 μL, Reno). For drug treatment, the mode of administration and concentration of drugs was described in figures. Monitoring of luciferase-expressing tumors was done using the Xenogen IVIS spectrum imaging system by injecting mice with D-Luciferin Firefly (YEASEN). Animals were monitored daily and euthanized upon displaying signs of distress or a ≥20% weight loss (whichever occurred first). Kaplan-Meier curves were created according to the survival results.

For the PDX model, 6-week-old BALB/c-nude male mice were intracranially implanted 5×10^5 tumor cells suspension. Mouse brain MRI images were then acquired, and tumor size was analyzed before and after treatment. Treatment strategy was carried out in accordance with figures.

Western Blot Analysis

Cells were harvested, washed with 0.9% NaCl, resuspended in TNTE buffer (50 mM Tris-HCl, 150 mM NaCl, 1 mM EDTA (pH=8), 1%Triton X-100, 25 mM NaF, 1mM Na_2VO_3, 100 μg/mL DTT, 100 μg/mL) with 100 μg/ml PMSF, 1 μg/mL, aprotinin, 1 μg/mL leupeptin, 1 μg/mL pepstatin and centrifuged at 12,000 rpm, 4°C for 30 min. Protein samples were analyzed by SDS-PAGE and electro-transferred to a Nitrocellulose (Pall). The blots were then blocked in 5% non-fat milk in TBST, followed by incubation of primary antibodies at 4°C overnight. After washing, the blots were incubated in horseradish peroxidase (HRP) conjugated secondary antibodies at room temperature for 1-2 h. Signals were detected using ECL (NCM biotech). The primary antibodies used are as follows: P21 (10355-1-AP, proteintech), Caspase3 (9665, CST), Cleaved-Caspase3 (9661, CST), PARP (9542, CST), Cleaved-PARP (9541, CST), GPX4 (30388-1-AP, proteintech), P53 (21891-1-AP, proteintech), GAPDH (10494-1-AP, proteintech).

Apoptosis Analysis

Apoptosis was detected using Annexin V-FITC Apoptosis Detection Kit (C1062, Byotime) according to the manufacturer's instructions. In brief, cells were collected and 1×10^5 to 1×10^6 cells were resuspended in 195 μL Annexin V-FITC-binding buffer. 2.5 μL of the Annexin V-FITC conjugate was added to each cell suspension and 5 μL of the 1mg/mL Propidium was then added to each cell suspension. Cells were analyzed on cytoflex (Beckman). The Clo-treatment concentration has limited effect in non-senescent cells (40 μM in LN229 and GL261).

RT-qPCR

RNA was collected for real-time qPCR analysis using the TRIzol reagent (15596026CN, Invitrogen). RNA was reverse transcribed using HiScript II Q RT SuperMix for qPCR (R323-01, Vazym). qPCR was performed with SYBR green-containing PCR kit (RR420A, Takara). Real-Time PCR System (Biorad) was used for data analysis. Primers used for qPCR are listed in Supplementary Table S1.

Cell Senescence Induction, β-Galactosidase Staining, and Senescence Probe

As described previously,[21] the senescent LN229 cells were induced by 50 μM TMZ for 4 days or 100 nM DOX for 4 days. The senescent U87MG cells were induced by 100 μM TMZ for 5 days or 100 nM DOX for 3 days. The senescent T3-5 and GL261 cells were induced by 300 μM TMZ for 5 days or 100 nM DOX for 3 days. Clo was applied to senescent cells for 24 h. LN229 and T3-5 cells were stained for β-galactosidase activity using a SA-β-Gal Stain Kit (G1508, solarbio). Images were then immediately captured using the EVOS FL Auto2 system. The acquired images were analyzed using the Image J. All samples were analyzed in triplicate with ≥3 fields per well. And the senescent level of GL261, LN229, T3-5 cells were examined using a CellEvent Senescence Green kit (C10841, Invitrogen).

Immunohistofluorescence

Brain tissues were fixed in 4% paraformaldehyde (PFA) overnight and dehydrated in 25% sucrose, then embedded in paraffin for IHF. The experiment was performed as described previously. After washing with 1×PBS three times, the slides were blocked in 5% sheep serum for 45 minutes, then probed with primary antibodies, P21 1:200 (10355-1-AP, proteintech), P53 1:500 (21891-1-AP, proteintech), Cleaved-caspase3 1:500 (9664, CST), Ki67 1:1000 (ab15580, Abcam) and incubated overnight at 4°C in a wet box. After washing with 1×PBS three times, the fluorescently-labeled secondary antibodies were incubated for 2 h at room temperature. The nuclei were visualized with DAPI (Sigma-Aldrich). Images were captured using a confocal laser scanning microscope (FV1000MPE-BX61WI, Olympus) and were analyzed using Image J software.

SiRNA and Plasmid Transfection

The P53 siRNAs were purchased from Tsingke Biotech Corporation. The human P53 siRNA sequences were: si1#: CCGGACGAUAUUGAACAAU, si2#: GGAAGACUCCAG UGGUAAU, si3#: GAUAUUGAACAAUGGUUCA. The mouse P53 siRNA sequences were: si1#: GAAUGAGG CCUUAGAGUUA, si2#: CCAUCUACAAGAAGUCACA, si3#: CGACCUAUCCUUACCAUCA. LN229 cells were transfected with siRNA via INTERFERin (PolyPlus PT-409-10) when the cells reached 70% to 80% confluency. For the wild type P53 and mutant P53 overexpression, the P53 cDNA and cDNA with Asn-288 deletion, Glu-349 deletion, R175H missense, R248Q missense or R273C missense, were insert into pcDNA3.1 vector via a ClonExpress MultiS One Step Cloning Kit (Vazyme). LN229 and U87MG was transfected with plasmid using LIPOFECTAMINE 3000 (Invitrogen).

Cellular Thermal Shift Assay

Cells were inculpated with DMSO or Clo for 1 hour and then digested as cell suspension in PBS to equally divide into few tubes, followed with heating under different temperature. Three snap freeze-thaw cycles were then performed to lyse cells, and protein was detected by Western blot analysis.

Surface Plasmon Resonance

The binding affinities of Clo for GST and its target proteins GST-P53 were assayed by SPR-based Biacore 1S+ instrument (cytiva). The CM5 sensor chip was used to immobilize target protein to the sensor surface by the standard amine coupling reaction at 25°C in PBS running buffer. Gradient concentrations of Clo containing 5% DMSO were injected into the channels to evaluate the binding affinity.

Single-Cell RNA-Sequencing

Tumor tissues were isolated into single-cell suspensions and performed on the 10X Genomics platform (CapitalBio Technology). The scRNA-seq dataset represents pooled tumors from three mice per group and was primarily used for exploratory and hypothesis-generating analyses. Similar pooling strategies have been reported in previous single-cell studies aiming to increase cellular yield and reduce technical variability, particularly when the primary objective is to identify transcriptional states rather than to perform replicated quantitative comparisons.[22,23] We aligned the data with mm10-2020-A, followed by barcode counting and unique molecular identifier (UMI) counting, to generate a raw gene expression matrix. Then, the expression matrix was converted to Seurat objects by the Seurat package in R 4.2.0 for further analysis and we randomly extracted appropriate cell from each group. By filtering cell with gene numbers (nFeature_RNA) < 300 and >7,500, UMI counting > 100,000, percentage of red blood cell genes >3% and percentage of mitochondrial genes >10%, the seurat object including 4,175 cells of control and 4,084 cells of Clofoctol. By "NormalizeData" function, cell gene expression from two group were normalized to a log scale and 3,000 highly variable genes from the normalized expression matrix were identified by 'FindVariableFeatures' function. Then, the "FindClusters" functions with top 15 principal components (PCs) and resolution 0.3 were used and identified 12 clusters. According to specific gene of each cluster (Supplementary Table S2), we annotated these cells as 7 cell types. See Supplementary Materials and Methods for InferCNV, hdWGCNA, and SIT details.

RNA-Sequencing

We cultured control, TMZ-induced (TMZ), and Clo-treated TMZ-induced (TMZ+Clo) LN229 and GL261 cells in triplicate, respectively, and extract the total RNA to created libraries for RNA-sequencing. Briefly, using oligod (T) beads, mRNAs were purified and fragmentated to target length range for generating cDNA libraries which were sequenced after clustering. We identified gene with $P<.05$ as the differentially expressed genes (DEGs) of TMZ vs control and TMZ+Clo vs TMZ. Gene Set Enrichment Analysis (GSEA) enrichment analysis was performed for DEGs to identify the influence of TMZ and Clofoctol for gene sets by R package "GSEABase." The GSVA algorithm was applied to explore the activity variation of hallmark gene sets by R package "GSVA" in LN229 and GL261 glioma cells. The differentially enriched gene sets of TMZ vs control and TMZ+Clo were identified with R package "limma". The DEGs were listed in Supplementary Tables S3-S6.

Protein-Protein Interaction Network

All the DEGs were retrieved in the STRING database to obtain the protein-protein interaction network, the species was set as "Homo sapiens," and the "medium confidence" was set at 0.5. At the same time, hide disconnected nodes in the network. The visualization of the PPI network was performed via Cytoscape 3.10.1 software.

Statistical Analysis

Results were performed on GraphPad Prism 8.0 and presented as the mean ± SDs. For two comparisons, Student's t test was used, and for three or more groups, one-way ANOVA was appropriately used to analyze experiment statistics unless otherwise stated. Dose-response curves for IC_{50} calculation and relative protein integrated density-temperature curve were calculated and draw by nonlinear fitting with appropriate parameters. Kaplan-Meier survival curve was analyzed by Mantel-Cox log-rank test. The MRI images and IHF images of tumor were measured by Image J. Not mentioned statistics are described in figure legends.

Results

scRNA-seq Revealed That Clofoctol Treatment Induced Significant Alterations in the Functional States of Tumor Cells

To explore change of GBM cells functional states response to Clo, we leveraged the GL261-luc cells to establish an orthotopic glioma model in C57BL/6J mice, and treated mice with saline and clofoctol as described in Figure 1A. Clo exhibited an obvious antitumor effect after 10 days of treatments (Figure 1B and C). We then performed scRNA-seq on tumors harvested from mice at day 10 post-treatment. Uniform manifold approximation and projection (UMAP) dimension reduction was performed on cells from two group (control and clofoctol) (Figure 1D), revealing a total of 12 clusters (Figure 1E). These clusters were identified as 7 cell types with distinct gene expression signatures (microglia cell, endothelial cell, neutrophils, B cell, T cell, macrophage, and glioma cell) and one not defined cell type (ND) (Figure 1F and Figure S1A). Moreover, consistent with

their malignant feature, glioma cells (cluster 0, 3, 6) demonstrated pronounced somatic copy number alterations, including chromosomal gains/losses at chromosome 5 and 15 (Figure S1B). Notably, Clo treatment reduced the CNV burden score in glioma cells, suggesting an effect on genome stability (Figure S1C).

As we previously described,[14] Clo treatment demonstrated significant anti-tumor effects in GBM through multiple mechanisms: (1) suppression of stemness properties, as evidenced by targeting glioma stem cells; (2) inhibition of cellular proliferation; and (3) induction of apoptosis, confirmed by increasing KLF13. We employed the AUCell algorithm to quantify single-cell pathway activity scores within glioma cell clusters, evaluating key functional states of tumor progression including: GSC, invasion, proliferation, apoptosis, and senescence signatures (Supplementary Table S7). Quantitative analysis revealed distinct patterns across treatment conditions, with Clo-treated cells showing significantly decrease in GSC, invasion, and proliferation (Figure 1G, Figure S1D). It is interesting to note that Clo treatment induced a reduction in senescence score in glioma cells (Figure 1G).

hdWGCNA and SIT Identified That Clofoctol Treatment Might Impede GBM Senescence

Since Clo-treatment could decline the senescence score in glioma cell, we then performed hdWGCNA and SIT to further analyze the senescence level of glioma cell. Utilizing hdWGCNA, a total of 15 network modules were identified based on soft threshold 6.0 (Figure S2A and B). Among these, 9 modules were correlated with Clo-treatment, including M1, M2, M3, M6, M7, M8, M10, M13, and M14 (Figure S2C). Gene signature scores across 9 functional modules associated with Clo treatment were computed in single cells using "Seurat" method (Figure S2D). We then used the hub genes of 9 modules for pathway enrichment analysis in which module 7 showed strong enrichment in P53 signaling pathway, DNA repair, cellular senescence, and cell cycle (Figure S2E and F) and this senescence-related module 7 was negatively enriched in Clo-treated versus controls (Figure S2G). Then we calculated the senescence score of module 7-related cells and found the score declined in Clo group (Figure S3A).

We then applied SIT on glioma cell to distinguish senescent cells from not senescent cells, and examined the proportions of senescence cell in two group based on senescence signature (Figure S3B), cell cycle arrest signatures (Figure S3C) and senescence score (Figure S3D). Compared with the control group, Clo treatment reduced the proportion of senescent cells to a certain extent (Figure S3E and F). Next, we isolated senescent glioma cells using SIT. In senescent glioma cell, the senescence-related genes and SASP genes expression were lower with Clo-treated (Figure S3G and H). Overall, the scRNA-seq analysis indicated that Clo could reduce the senescence of glioma cells.

Clofoctol Inhibited Glioma Cell Senescence In Vitro

To verify anti-senescence effect of Clo, three senescent glioma cell models (GL261, LN229, T3-5) were constructed by using temozolomide (TMZ) and doxorubicin (DOX) as before.[21] Across all models, TMZ/DOX treatment elevated senescence-associated beta-galactosidase (SA-β-Gal) activity compared to controls, while Clo treatment reduced these signals (Figure 2A). We also detected that Clo treatment reduced the percentage of SA-β-Gal-positive GBM cells treated with TMZ or DOX in LN229 and T3-5 cells (Figure 2B). When performing Clo on senescent glioma cell and not senescent cell, Clo prioritized inhibiting cell viability of senescent cells over not senescent cell (Figure S4A and B). And expression of some senescence related genes in LN229 (*CDKN1A*, *CDKN2A*, *CSF1*, *CSF3*, *CXCL15*, *TGFB1*, *BMP2*) and GL261 (*Cdkn1a*, *Cdkn2a*, *Csf1*, *Csf3*, *Csf2*, *Cxcl13*, *Cxcl15*, *Bmp2*, *Tgfb1*, and *Mmp3*) were stimulated by TMZ, which inhibited by Clo instead (Figure 2C). Clo attenuated TMZ/DOX-induced P21 upregulation in GL261, LN229, and T3-5 cells (Figure 2D).

To validate whether Clo impeded glioma cell senescence by directly killing senescent cells or reversing cellular senescence, pharmacodynamic analysis of Clo was performed in GL261 and LN229. We performed Clo on glioma cell before or after TMZ or DOX-induction, resulting that senescent cells were more sensitive to Clo than non-senescent cells (Figure 2E). Inversely, when we performed TMZ on TMZ- or DOX-induced glioma cell, Clo-treatment did not promote cell sensitivity to TMZ, which indicated Clo couldn't reverse cellular senescence (Figure S4C and D). Collectively, our results demonstrated that Clo effectively eliminates TMZ/DOX-induced senescent glioma cells.

Clofoctol Stimulated the Death of Senescence Glioma Cells through Ferroptosis and Apoptosis

To elucidate how Clo eliminates therapy-induced senescent glioma cells, we performed comprehensive RNA sequencing across three experimental groups: (1) proliferating tumor cells (control), (2) therapy-induced senescent tumor cells (TMZ), and (3) senescent tumor cells following Clo treatment (TMZ+Clo) to systematically characterize transcriptional changes associated with Clo-mediated senolysis. The differential gene expression (DEG) analysis defined 953 upregulated and 802 downregulated genes in senescent LN229 cells compare to control with P value < .05 while we defined 743 upregulated and 1411 downregulated genes in Clo-treated senescent LN229 compared to senescent LN229 cells (Figure 3A). The same analysis was performed on GL261 and we got 38 upregulated and 58 downregulated genes in senescent GL261 induced by TMZ, 1348 upregulated and 1193 downregulated genes in Clo-treated senescent GL261 (Figure S5A). Gene set enrichment analysis (GSEA) was implemented to identify enriched pathways in senescent LN229 cells compared with control, we found that the DEGs were positively enriched to anti-apoptotic TRAIL signaling (APOPTOSIS_VIA_TRAIL_DN, NES = 1.37, P = .04) and negatively enriched to pro-apoptosis TRAIL signaling (APOPTOSIS_VIA_TRAIL_UP, NES = –3.44, P = 3.84E–64) (Figure 3B). However, Clo treatment significantly enhanced pro-apoptotic signaling (APOPTOSIS_VIA_TRAIL_UP, NES = 3.35, P = 1.64E–102) while suppressing anti-apoptotic mediators (APOPTOSIS_VIA_TRAIL_DN, NES= –1.96, P = 2.65E–06) in senescent glioma cells (Figure 3B). The GSEA result of GL261 also showed the Clo positive regulated apoptosis-related pathways, including apoptotic

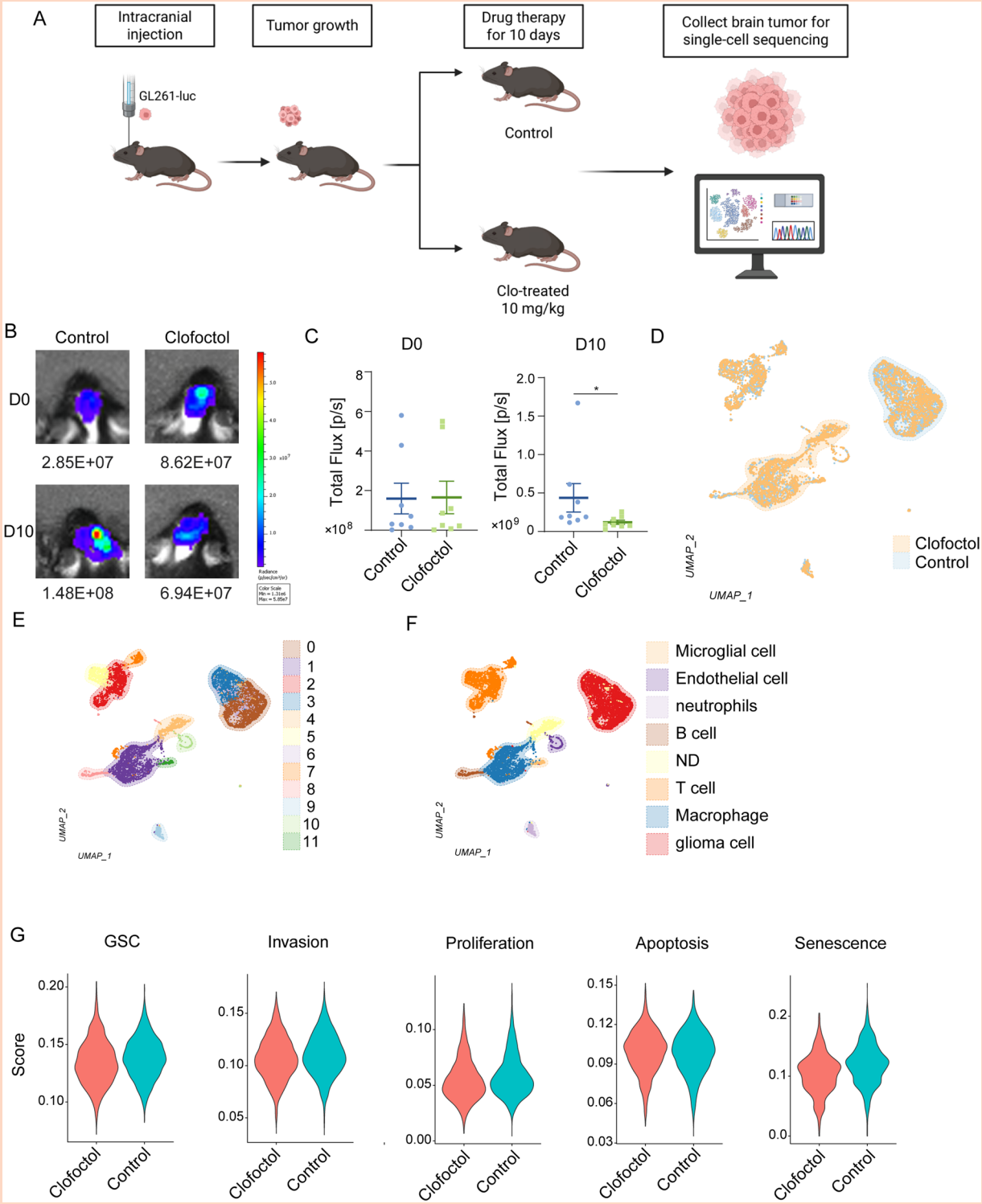

Figure 1. scRNA-Seq of GL261-derived tumor in C57BL/6J mice. (A) Schematic of the single-cell sequencing workflow: Mice with GL261-luc orthotopic tumors were divided into two groups: Control administered with 0.9% normal saline via tail vein injection and clofoctol-treated (Clo-treated) administered with 10 mg/kg clofoctol for 10 days. Tumors were then harvested and processed for single-cell RNA sequencing. Figure created by BioRender.com. (B, C) The representative luciferase images (B) and total flux [P/S] of mice on D1 and D10 from treated (C) (mean ± SEM, $n = 8$). The unpaired Student's t-test determined the significance level. *$P < .05$. (D) UMAP visualization colored by sample. (E) UMAP visualization colored by Seurat_clusters. (F) UMAP visualization colored by cell type in clofotcol and control group. (G) VlnPlot showing AUCell score of cell functional status gene sets in Clo-treated and control glioma cells.

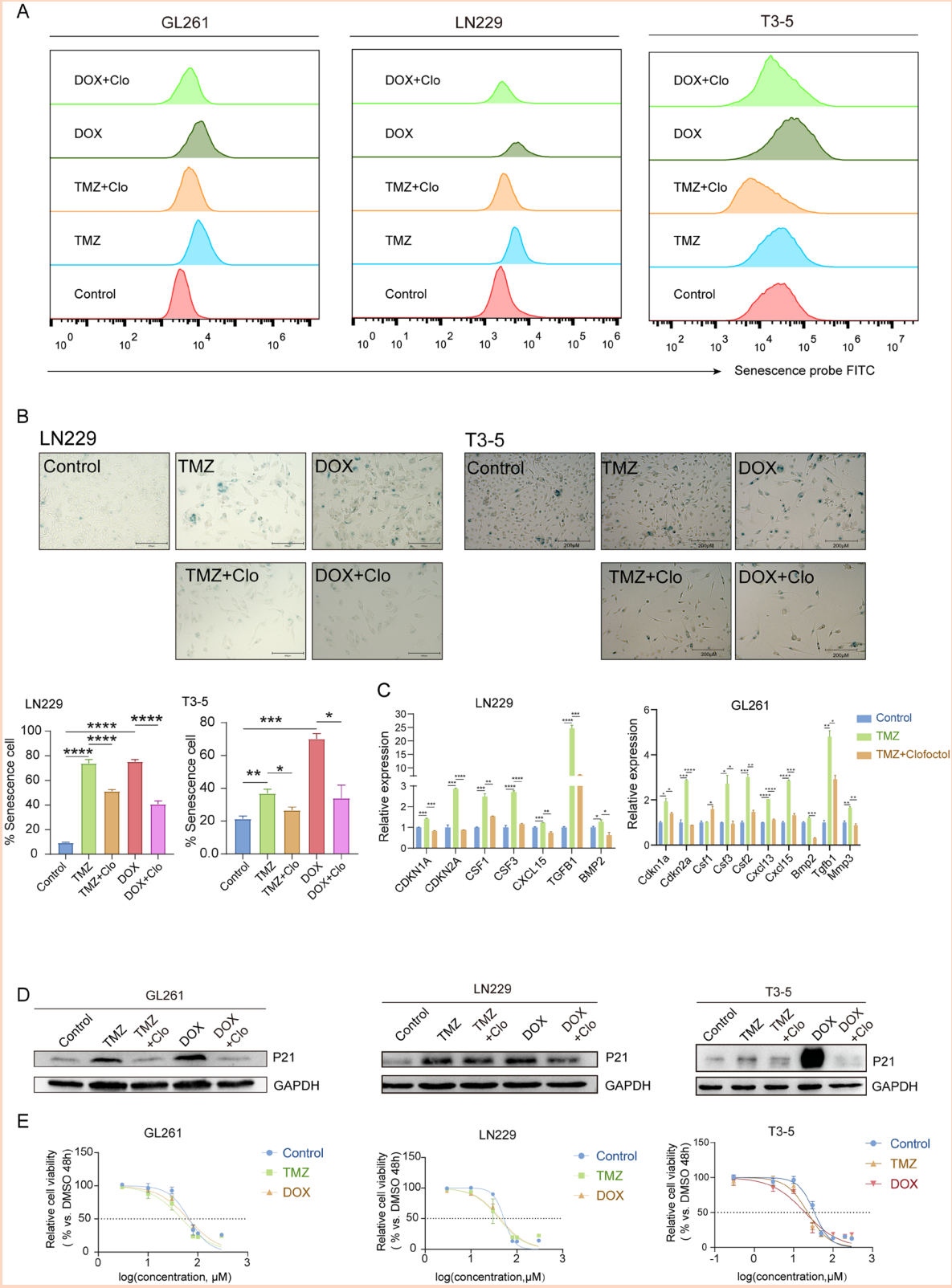

Figure 2. The clofoctol is more sensitive to senescent glioma cells. (A) Cellular senescence was measured by flow cytometry via senescence probe staining. (B) SA-β-gal was assessed via X-gal staining in glioma cells. Scale bar 200 μm. $^{*}P < .05$, $^{**}P < .01$, $^{***}P < .001$, $^{****}P < .0001$ by one-way ANOVA with Tukey's multiple comparison test. (C) RT-qPCR analysis of SASP genes in glioma cells. The data are presented as the means ± SDs. $^{*}P < .05$, $^{**}P < .01$, $^{***}P < .001$, $^{****}P < .0001$ by one-way ANOVA with Tukey's multiple comparison test. (D) Western blot analysis of P21 protein in GL261, LN229, and T3-5 cells. (E) Dose-response curves for Clofoctol in senescent glioma cells.

signaling pathway in response to DNA damage by p53 class mediator, intrinsic apoptotic signaling pathway in response to endoplasmic reticulum stress and apoptosis by serum deprivation up (Figure S5B). Meanwhile, the GSEA result also proved that Clo positively regulated the gene of ferroptosis in senescent LN229 (Figure 3C).

Furthermore, we measured cell apoptosis induced by Clo in senescent glioma cells in vitro. Flow cytometry analysis revealed Clo induced significantly apoptosis in senescent glioma cells than non-senescent glioma cells (Figure 3D) and Western blot analysis showed that Cleaved-Caspase3 and Cleaved-PARP were stimulated more strongly by Clo in senescent glioma cells (Figure S5C). To investigate Clo's impact on ferroptosis in senescent glioma cells, we measured key ferroptosis marker GPX4 protein. The experimental data demonstrated that Clo treatment downregulated the expression of GPX4 in TMZ- and DOX-induced senescent cells (Figure 3E). Next, we treated the TMZ-induced senescent glioma cells with the ferroptosis inhibitor Ferrostatin-1 (Fer-1) following Clo. The results demonstrated that Fer-1 upregulated GPX4 expression, and also reversing the Clo-mediated suppression of p21 expression (Figure 3F). The same result also was observed in DOX-induced senescent glioma cells (Figure S5D). Furthermore, senescence probe analysis revealed that Fer-1 counteracted the Clo-mediated suppression of senescence in TMZ- and DOX-induced glioma cell (Figure 3G and Figure S5E). In addition, Fer-1 could weak the sensitivity of TMZ- and DOX-induced senescent cell for Clo (Figure 3H and Figure S5F). Collectively, our findings demonstrate that Clo eliminates senescent cells through a dual mechanism involving the activation of both apoptotic and ferroptotic pathways.

Clofoctol Induce Senescent Cell Death by Binding P53

Our findings that senescent glioma cells exhibit marked sensitivity to Clo led us to postulate that the therapeutic target responsible for triggering both apoptotic and ferroptotic pathways is preferentially expressed in the senescent cell. We next applied the GSVA algorithm to assess the pathway activity (referred to as GSVA score) of each hallmark gene sets in LN229 cells across three groups: Control, TMZ-treated, and TMZ+Clo. Within the top 20 gene sets (ranked by *P* value), the P53 signaling pathway ranked second, demonstrating strong activation (high GSVA score) under TMZ treatment but significant suppression (low GSVA score) with TMZ+Clo combination therapy (Figure 4A). We then drawn the PPI network of the DEGs of TMZ+Clo compared to TMZ using Cytoscape 3.10.1 to search the target gene of Clo in senescent glioma cells. PPI analysis showed P53 occupied the core position with the top1 degree (Figure 4B, Supplementary Table S8). Based on this, P53 was considered the hub genes. To characterize the potential binding mode, we applied AutoDock vina to perform molecular docking on the active site of P53 and Clo to assess their binding activity. The result showed the minimum binding energies (refer to the Affinity value) between Clo and P53 was –5.6581 kcal/mol and Clo interact with the Asn-288 and Glu-349 of P53 through hydrogen bonds (Figure 4C). Next, P53 protein expression was assessed by Western blot, in which P53 was upregulated in TMZ- and DOX-induced senescence but downregulated in Clo-treated senescent glioma cells (Figure S6A). When we eliminated the Asn-288 and Glu-349 from P53, the absolute affinity value of Clo and P53 was decreased and there are no more hydrogen bonds between Clo and P53 (Figure S6B and C). To verify the prediction above, CETSA was used to show that with Clo protection, P53 was more stable compared to control in TMZ-induced senescent glioma cell (Figure 4D). We further tested P53 stability under temperatures from 25 to 72°C in DOX-induced senescent glioma cell (Figure S6D) and non-senescent glioma cell (Figure S6E). The results showed that in senescent glioma cell, Clo could protect P53 from degradation while in non-senescent glioma cell, the protection for P53 was not apparent, which suggested Clo strongly bind P53 in senescent glioma cell. The direct interaction between Clo and p53 was evaluated by surface plasmon resonance (SPR), yielding a dissociation constant (Kd) of 52.2 μM, indicating a moderate micromolar-range binding affinity. Notably, GST alone exhibited substantially weaker binding to Clo (Kd = 789 μM), supporting the presence of a p53-specific component in the observed interaction (Figure S6F). Next, to pinpoint specific Clo's binding site on P53, we constructed two deletion mutants (P53-Δ288 and P53-Δ349) and analyzed their thermal stability over a range of temperatures (25-72°C). The results proved that Clo protected WT-P53 and P53-Δ349 but not P53-Δ288 in LN229 cells (Figure 4E and Figure S6G), indicating that Asn-288 was the key binding site of P53 and Clo. To evaluate the potential of Clo in targeting P53-mutated tumors, we performed molecular docking with three common hotspot mutants: R175H, R248Q, and R273C.[24] The analysis revealed that Clo maintained a binding affinity comparable to that of wild-type p53 (–5.658 kcal/mol), with binding energies of –5.018 kcal/mol (R175H), –5.345 kcal/mol (R248Q), and –6.164 kcal/mol (R273C) (Figure S7A) and the Clo still preferentially killed senescent cell in U87MG overexpressed the three P53 mutants (Figure S7B). Notably, R175H and R248Q inhibited the preferential killing effect of Clo to some extent (Figure S7B). To further validate P53 function on Clo target senescent glioma cell, we used siRNAs to knockdown P53. The GL261 siRNA-1# and LN229 siRNA-3# presented obvious P53 knockdown activity (Figure S7C) and were used for the following experiments. Using senescence probe, the senescence level increased again after Clo-treatment when P53 was knocked down in TMZ or DOX-induced glioma cells (Figure 5A and Figure S7D). By Western blot analysis, we also found that knocking down P53 promoted GPX4 protein in TMZ or DOX-induced glioma cells with Clo-treatment (Figure 5B and Figure S7E). In apoptosis analysis, knocking down p53 decreased the Clo-induced apoptosis cell proportion in senescent glioma cells (Figure 5C). Then, a p53 lentiviral knockdown LN229 was constructed (Figure 5D) on which Clo had lower suppressive effects after TMZ- and DOX-inducement compared to LN229-shNC (Figure 5E and F). Above all, our data suggested that, in senescent glioma cells, Clo-triggered apoptosis and ferroptosis were p53-dependent.

Combined TMZ and Clofoctol: An Effective Treatment Strategy

The foregoing results motivated us to validate the Synergistic anti-GBM effect of TMZ and Clo. We analyzed the combination

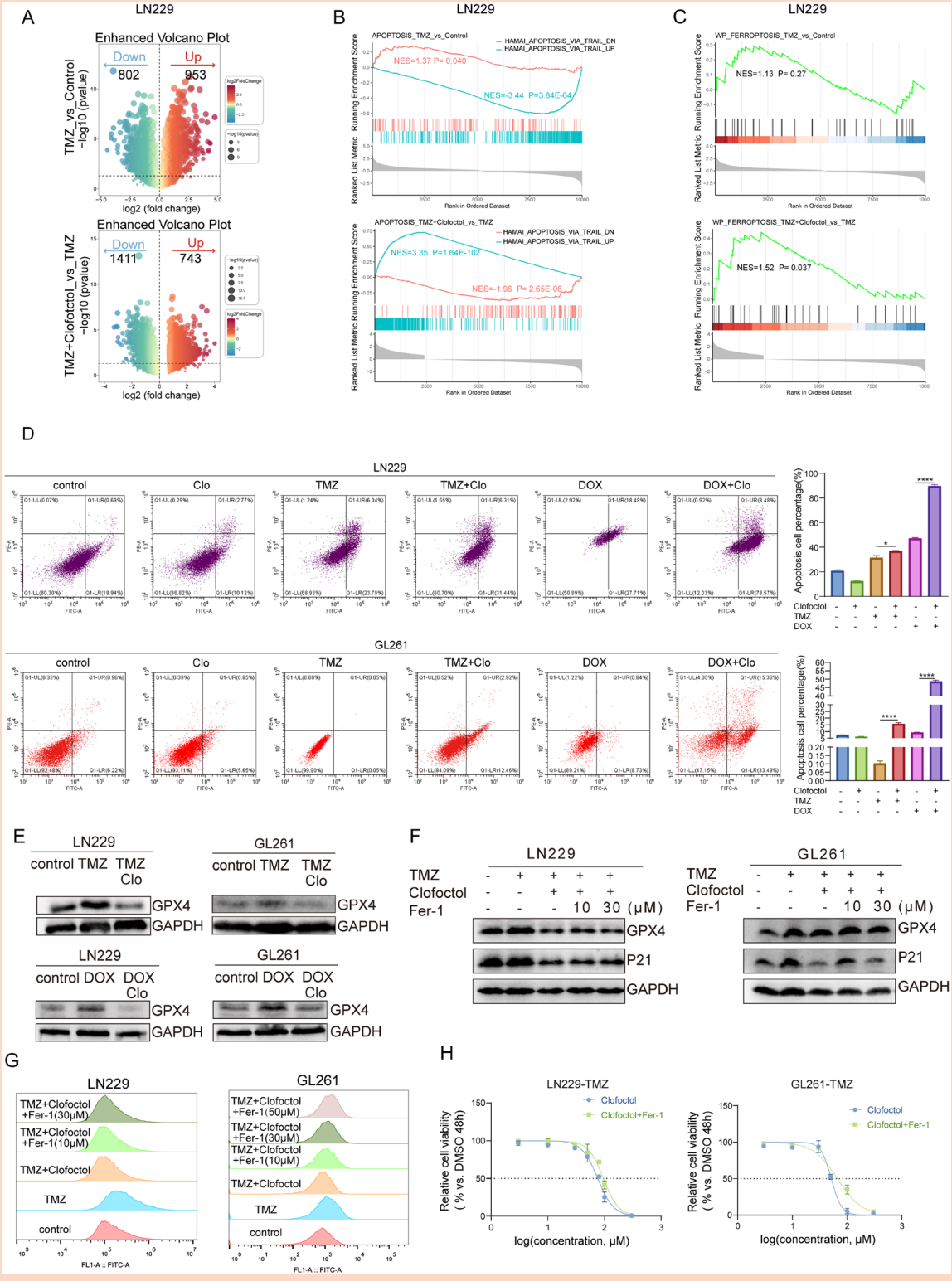

Figure 3. RNA sequencing reveals mechanism by which clofoctol promotes cell death in senescent glioma cells. (A) Volcano Plot of differential gene expression analysis of TMZ vs Control (upper) and TMZ+Clofoctol vs TMZ (lower) in LN229. (B, C) Gene set enrichment analysis (GSEA) identifies signaling pathways associated with apoptosis (B) and ferroptosis (C) involved in differential gene of TMZ vs Control (upper) and TMZ+Clofoctol vs TMZ (lower). (D) Flow cytometry analysis of apoptosis cell in senescent and non-senescent glioma cells treated with Clo. The data are presented as the means ± SDs. *$P < .05$, ****$P < .0001$ by one-way ANOVA with Tukey's multiple comparison test. (E) Western blot analysis of GPX4 protein in Clo-treated senescent glioma cell. (F) Western blot analysis of P21, GPX4 proteins in Clo-treated senescent glioma cells and Fer-1+Clo-treated senescent glioma cells. (G) Cellular senescence in Clo-treated senescent glioma cells and Fer-1+Clo-treated glioma cells was measured by flow cytometry via senescence probe staining. (H) Dose-response curves for Clo in senescent glioma cells and Fer-1-treated senescent glioma cells induced by TMZ.

index (CI-index) of TMZ and Clo in vitro and found TMZ and Clo exhibited strong synergistic inhibitory effect (Figure S8A-C). Moreover, we administrated PDX- and GL261-derived orthotopic tumor mice models with saline (Control), temozolomide (TMZ), Clofoctol (Clo), combination of TMZ and Clofoctol (TMZ+Clo) (Supplementary File, Figure S8D). In PDX models, TMZ+Clo further inhibited tumor growth rates in brain (Figure 6A) and IHF showed Ki67-positive cells decreased and Cleaved-Caspase3-positive cells increased in TMZ+Clo compared to TMZ group (Figure 6B and C). Moreover, the P21-positive and P53-positive cell in TMZ were declined in TMZ+Clo (Figure 6D and E). In GL261 models, TMZ+Clo also further inhibited tumor growth in vivo (Figure S8E). To predict the therapeutic outcomes, the mice weight and survival after treatment were also explored. TMZ+Clo better maintained mouse weight over the period of treatment (Figure S8F) and TMZ+Clo treatment further extended mouse survival compared to TMZ alone (Figure 6F). We then measured the senescence cell proportion in tumors, the result showed after TMZ treatment, senescent cells increased while the combination treatment reduced the number of senescent cells (Figure 6G). And IHF in GL261 models also showed P21-positive cells decreased in TMZ+Clo group (Figure S8G). These data demonstrate that the TMZ+Clo combination enhanced therapeutic efficacy against glioma and reduced tumor cellular senescence compared to TMZ alone. Summary of the proposed molecular mechanism is shown in Figure 6H.

Discussion

As an established high-resolution analytical platform, scRNA-seq enables comprehensive characterization of cellular states at the individual cell level. Through integrative multi-modal analysis combining scRNA-seq and hdWGCNA, we systematically characterized Clo's pleiotropic effects on tumor cell populations, with particular emphasis on its potent modulation of cellular senescence programs. We acknowledge that the scRNA-seq data was generated from pooled samples, which limits statistical power regarding biological variability. However, key findings were validated in independent cohorts.

In our previous work, Clo was defined as a GSC-targeted drug which binding upstream of N-ras (UNR), thereby inducing GSC apoptosis with minimal toxicity to normal cells and favorable blood-brain barrier (BBB) permeability. In mice, intravenous administration of Clo at 10 mg/kg resulted in measurable brain exposure, with brain concentrations reaching 152 to 187 ng/g within 5 to 90 minutes after the final injection, supporting its ability to penetrate the BBB in vivo.[14] Importantly, although direct measurements of human brain concentrations are limited, available clinical pharmacokinetic data indicate that Clo exhibits good systemic exposure in humans. Following a single rectal administration of 1.5 g, Clo achieved a mean plasma AUC of 112.78 μmol/L·h, demonstrating efficient absorption and sustained systemic availability.[25] Given Clo's physicochemical properties and its documented BBB penetration in mouse models, these pharmacokinetics (PK) characteristics support the plausibility that therapeutically relevant brain concentrations could be achievable under clinically feasible dosing regimens. In this study, we further extend this concept by showing that Clo exhibits limited cytotoxicity toward proliferating glioma cells but potently induces apoptosis in senescent glioma cells. This preferential vulnerability is consistent with our previous observations in GSCs and suggests that Clo may preferentially target stress-adapted or therapy-induced tumor cell states, thereby offering a mechanistically distinct and potentially complementary strategy for glioma treatment.

TMZ, the first-line therapeutic agent for GBM, is an oral alkylating chemotherapy drug that has demonstrated significant single-agent activity against GBM in clinical settings.[26,27] TMZ treatment mainly induces apoptosis.[28] However, approximately 50% of patients develop TMZ resistance, mediated through two distinct mechanisms: (1) intrinsic resistance conferred by MGMT expression in treatment-naive GBM cells, and (2) acquired resistance driven by dynamic genomic and epigenetic alterations in adapted tumor populations.[29] TIS represents a pivotal mechanism of TMZ resistance in GBM cells, with activation of the p53/p21 signaling axis and consequent G2/M cell cycle arrest serving as the primary molecular mediators.[30,31] The senescent cells also display resistance to apoptosis for the increased MGMT.[28,32] Above all, exploring senolytic drugs to kill senescent cell to prevent drug-resistance become a new sight for GBM.[33–35] However, current senotherapeutic strategies for cancer remain largely limited to Bcl-2 family protein inhibitors,[35,36] highlighting a critical need for alternative molecular target. In this study, we identified Clo as a p53-targeting compound that preferentially eliminates senescent glioma cells, simultaneously revealing its potential as a candidate senotherapeutic drug.

Ferroptosis is a unique modality of cell death driven by iron-dependent phospholipid peroxidation and regulated by xc–cystine/glutamate antiporter-GPX4 pathway, iron metabolism pathway and lipid metabolism pathway.[37] GPX4 catalyzes the reduction of PLOOHs in mammalian cells.[38] Disfunction of GPX4 causes excessive lipid peroxidation resulting as ferroptosis.[39] As a cell death mechanism different from apoptosis, necrosis and autophagy, ferroptosis is initially explores for cancer to invert the therapy-resistance. Tumors like Melanoma, ovarian cancer, non-small cell lung cancer and GBM resistant to apoptosis and common therapeutics are vulnerable to ferroptosis agonist, for the drug-resistance cells are highly dependent on GPX4 peroxidase activity for survival.[40–42] Moreover, many chemotherapy drugs have been proved could trigger ferroptosis.[43,44] We found Clo could lower GPX4 protein and its senolytic effect partially depends on ferroptosis, which was associated with P53.

As a transcription factor (TF), P53 hinders normal cell transformation by regulating cell cycle and proliferation, while in tumor cell, P53 frequently paly a complex role to bidirectionally regulated cell DNA stability, GSC self-renewal, cell senescence, cell death and other tumor progress processes.[45] Utilizing CETSA and SPR, we identified the interaction of Clo and P53 in vitro. Although the SPR-derived Kd was modest, the downstream response (apoptosis and ferroptosis) of Clo was substantially recovered by knocking down P53 and another Clo target UNR was found non-functional in senescent glioma cells (data not shown), which proved the specific functional relevance of P53 and Clo.

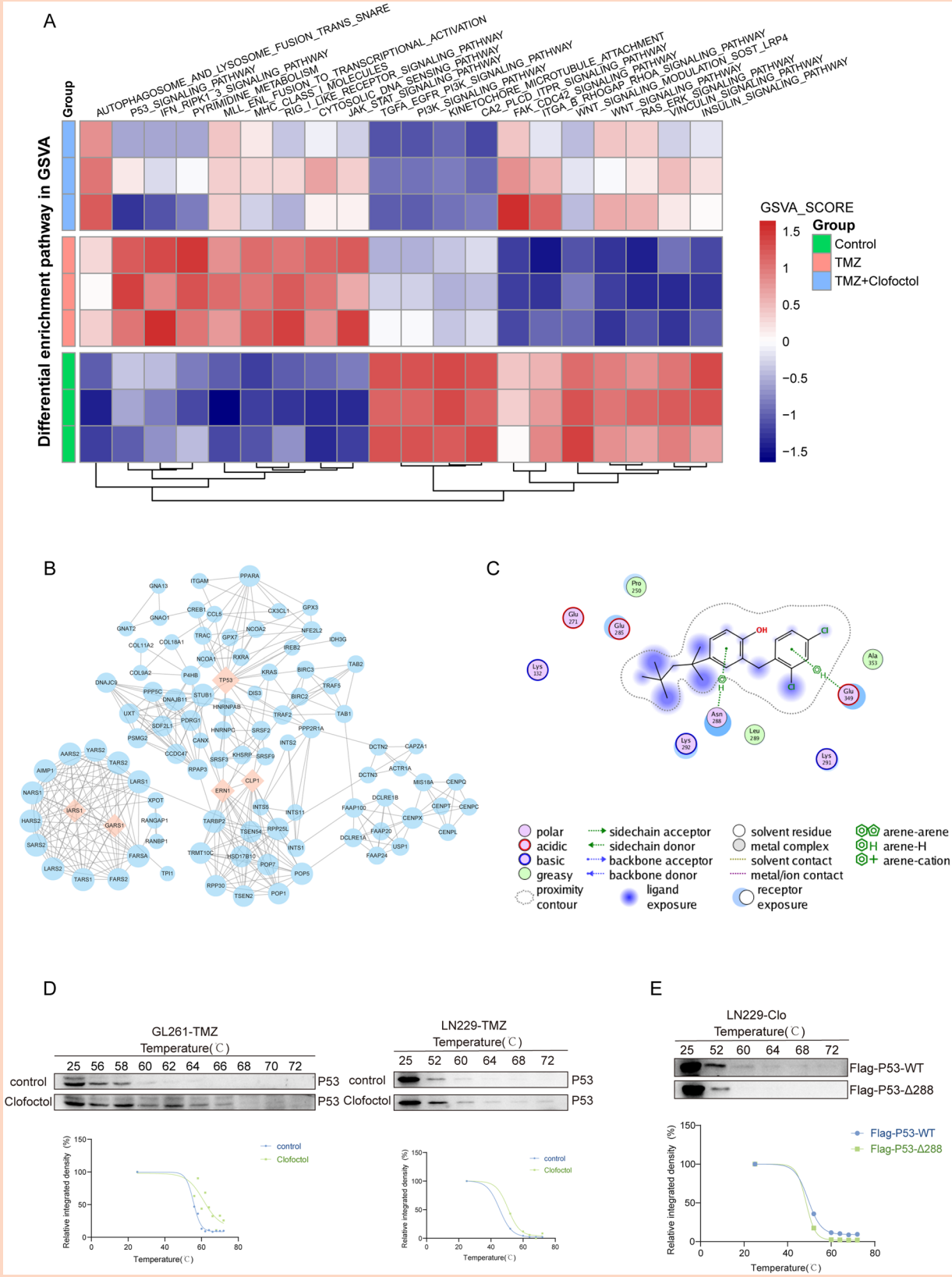

Figure 4. RNA-seq combined with molecular docking indicated P53 as potential targets of clofoctol. (A) GSVA_score heatmap of pathways identified in TMZ+Clofoctol vs TMZ by gene set variation analysis (GSVA). (B) The PPI network of DEG. (C) Molecular docking of Clo and P53. (D) Clo promoted resistance of P53 to different temperature gradients in senescent glioma cells, which was detected by CETSA. (E) Western blot showed the stronger protection of Clo for Flag-P53-wt than Flag-P53-Δ288 under different temperature gradients, which was detected by CETSA.

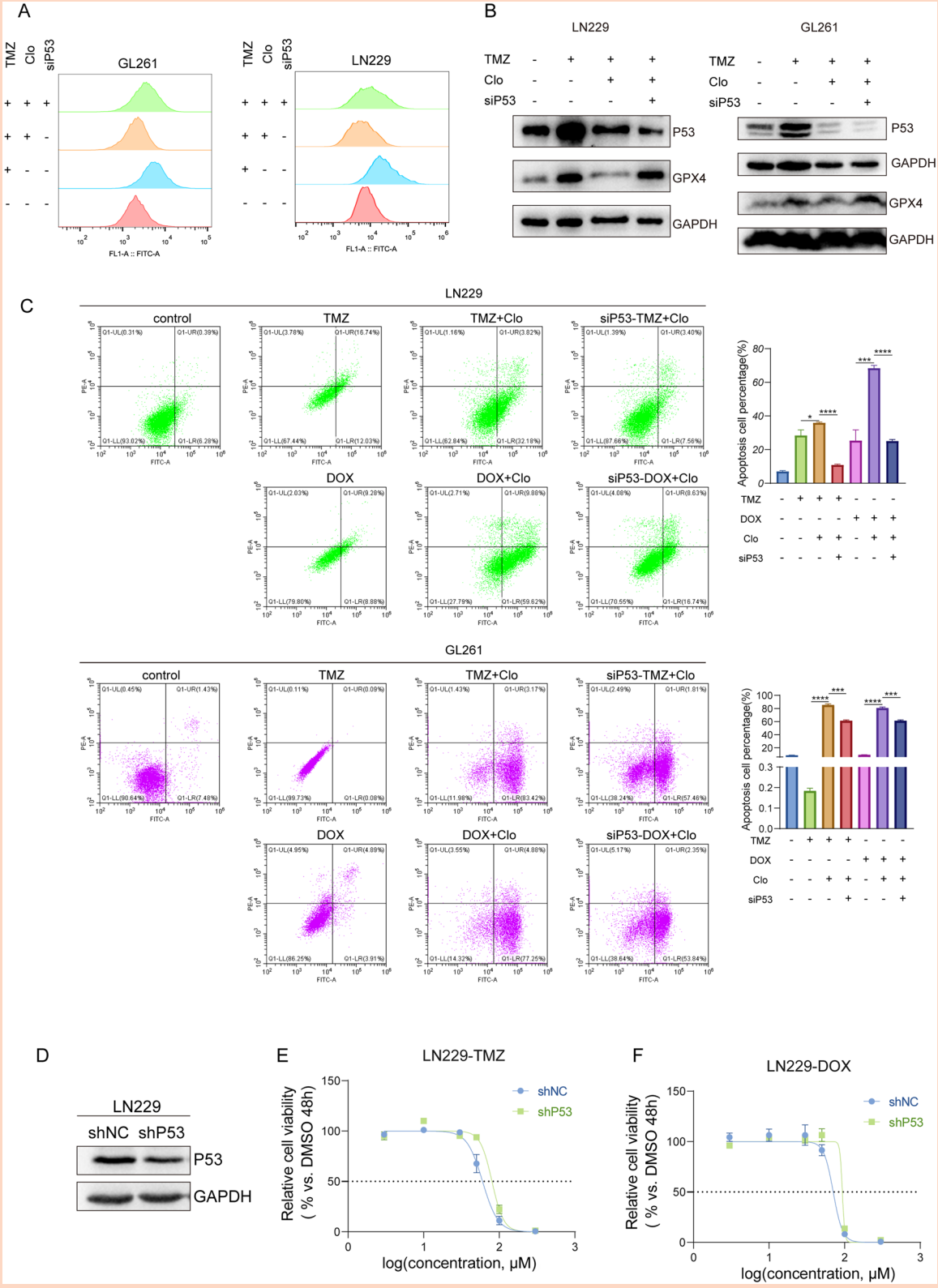

Figure 5. Clofoctol induces senescent glioma cells death by binding P53. (A) Cellular senescence in Clo-treated senescent glioma cells and Clo-treated P53 knockdown senescent glioma cells was measured by flow cytometry via senescence probe staining. (B) Western blot analysis of P53, GPX4 protein in Clo-treated senescent glioma cell and Clo-treated P53 knockdown senescent glioma cells. (C) Apoptosis cell in Clo-treated senescent glioma cells and Clo-treated P53 knockdown senescent glioma cells which was analysis by flowcytometry. The data are presented as the means ± SDs. $^{*}P < .05$, $^{***}P < .001$, $^{****}P < .0001$ by one-way ANOVA with Tukey's multiple comparison test. (D) Western blot analysis of P53 protein in P53 knockdown LN229 transfected with lentivirus (LN229-shP53). (E, F) Dose-response curves for Clofoctol in senescent LN229-shNC and senescent LN229-shP53.

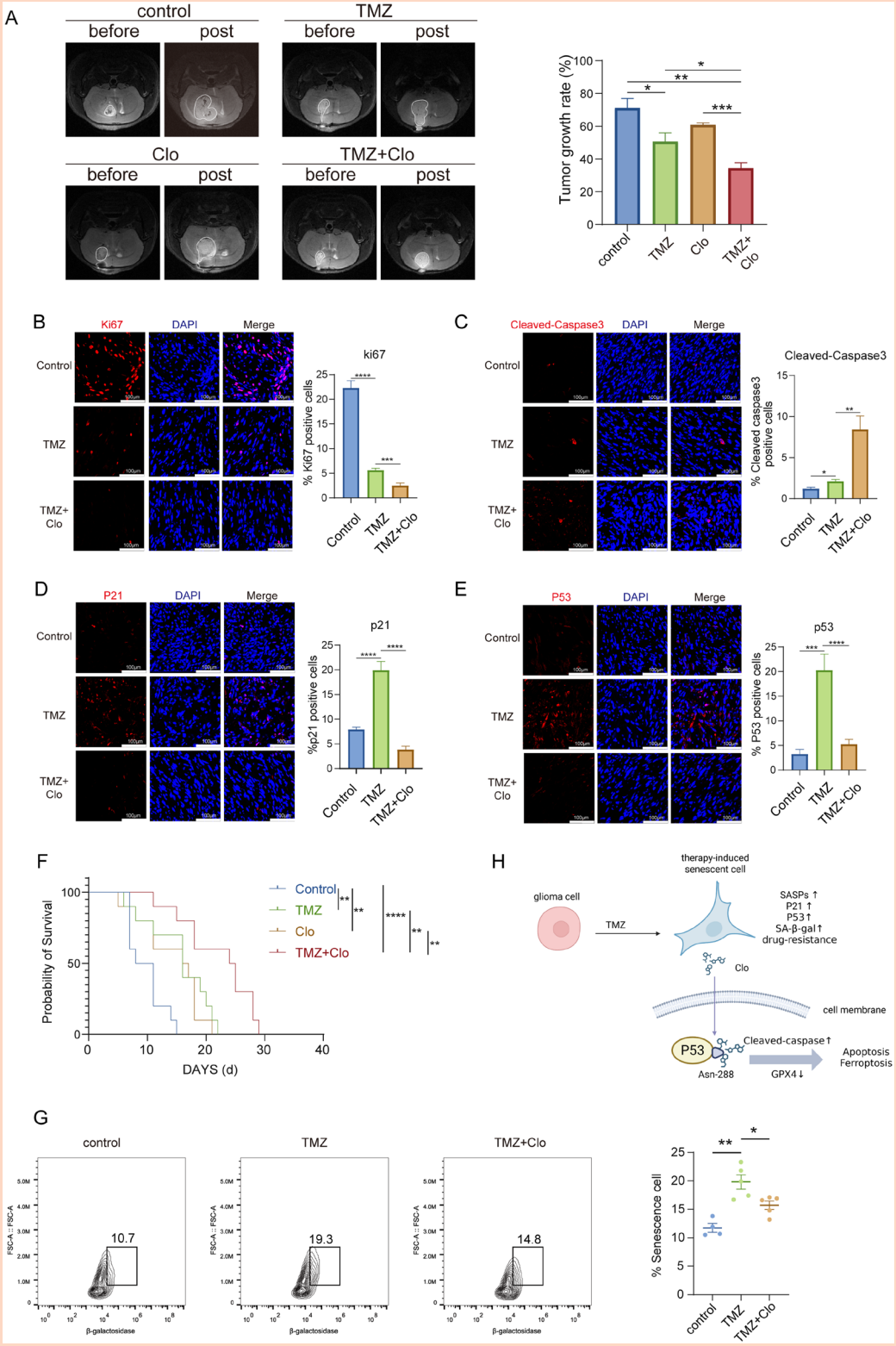

Figure 6. The combination of TMZ and clofoctol inhibited the growth of glioma in vivo. (A) The presentive MRI images and tumor growth rate of four groups. (B-E) Representative staining images of Ki67 (B), Cleaved-Caspase3 (C), P21 (D) and P53 (E) in the PDX-derived tumors treated with TMZ or TMZ combined with Clofoctol. Positive cells were quantitated and presented as a bar graph. *$P < .05$, **$P < .01$, ***$P < .001$ and ****$P < .0001$ by one-way ANOVA with Tukey's multiple comparison test. (F) the survival curves of Mice in four groups. The Mantel-Cox log-rank test was used for analysis, **$P < .01$ and ****$P < .0001$. (G) Proportion of senescent cells in tumors and the data are presented as means ± SDs. *$P < .05$, **$P < .01$ by one-way ANOVA with Tukey's multiple comparison test. (H) The senescent glioma cells induced by TMZ/DOX showed increased SASPs, P21, and P53 expression accompanied with SA-β-gal activity. Senescent cells could be caught by Clo through P53 and induced cell death via apoptosis and ferroptosis. Figure created by BioRender.com.

Numerous researches suggest that P53 mutation regulate malignant phenotypes by: (1) loss of function, (2) dominant negative effect and (3) gain of function. ~30% of samples from human primary GBMs harbor TP53 mutations, and in TMZ-resistant GBM cell lines, p53 gene mutations were found.[46] To determine whether the clinically relevant P53 mutations affect the function of Clo in senescent glioma cells, we employed molecular docking to evaluate the binding ability of Clo with three common hotspot p53 mutants in GBM: R175H, R248Q, and R273C. These mutations have a high incidence in GBM and have been confirmed to exhibit gain-of-function characteristics. In our study, the molecular docking analysis predicted Clo maintained binding capability with P53-R175H, P53-R248Q, and P53-R273C. Consistent with the predictions, Clo exhibited comparable preferential killing ability in senescent U87MG overexpressed P53-R273C and P53-WT, while P53-R248Q and P53-R175H likely hindered the biological function of Clo. These findings suggest that the therapeutic efficacy of Clo may extend to glioma patients with some clinically relevant P53 mutations. However, the mainly functional Clo target was still P53-WT. For mutant P53, further mechanistic studies using defined mutant model and clinical investigation are warranted.

The targets of Clo have been identified are multifarious in different situations. Clo binds Cdc7/Dbf4 protein complex in OEC-M1 oral cancer cells to arise UPR.[15] In GBM, UNR has been identified as the target of Clo and the B7 (a Clo derivatives with scaffold-oriented molecular optimization) binds CD155 to activate NK cell-mediated immunity.[14,47] We have demonstrated P53, a crucial protein regulating tumor process, was the Clo target in senescent glioma cell. In summary, Clo impedes GBM with multiple targets in many aspects, including targeting GSCs, modulating antitumor immunity and senescent cell. However, the direct p53-dependent mechanism of Clo prior to cell death remains unclear, warranting further investigation in vivo. Of note, human brain exposure of Clo has not been directly assessed, representing a limitation for clinical translation. Comprehensive preclinical pharmacokinetic and extended toxicology studies of Clo are therefore essential.

Supplementary Material

Supplementary material is available online at *Neuro-Oncology Advances* (https://academic.oup.com/noa).

Keywords

clofoctol | glioblastoma | scRNA-seq | p53 | senescence

Author Contributions

Yuxin Zhang: Conceptualization, Investigation, Methodology, Writing—original draft. Zhixing Wang: Methodology, Writing—review & editing. Yue Wang: Methodology, review & editing. Enyan Li: Methodology, review & editing. Fan Wu: Methodology, Data analysis. Lin Hou: Methodology, Investigation, Formal analysis. Bin Yin: Methodology, Investigation. Boqin Qiang: Conceptualization, Writing—review & editing. Wei Han: Supervision, Conceptualization, Funding acquisition, Writing—review & editing. Xiaozhong Peng: Supervision, Conceptualization, Funding acquisition Writing—review & editing.

Conflict of Interest Statement

The authors declare that they have no competing interests.

Funding

This work was supported by the National Key R&D Program of China (2022YFC3401000 and 2022YFA1103803), the National Natural Science Foundation of China (82173373), the CAMS Innovation Fund for Medical Sciences (CIFMS) grant (2021-I2M-1-034) and State Key Laboratory Special Fund (2060204).

Acknowledgments

We thank State Key Laboratory of Common Mechanism Research of Major Diseases Platform for consultation and instrument availability that supported this work. Figures 1A, S8D, and 6H were created using BioRender.com.

Ethics Approval

The related studies were approved by the institutional review board of Institute of Basic Medical Sciences, Chinese Academy of Medical Sciences (ZS2023007). All the animal studies were approved by the Institutional Animal Care Use & Welfare Committee of the Center for Experimental Animal Research (ACUC-A01-2022-059, ACUC-A02-2025-005).

Data Availability

All data used in this work can be acquired from the corresponding author upon reasonable request.

Affiliations

State Key Laboratory of Common Mechanism Research for Major Diseases, Department of Biochemistry & Molecular Biology, Institute of Basic Medical Sciences & School of Basic Medicine, Chinese Academy of Medical Sciences & Peking Union Medical

College, Beijing, China (Y.Z., Z.W., Y.W., E.L., L.H., B.Y., B.Q., W.H., X.P.); Department of Molecular Neuropathology, Beijing Neurosurgical Institute, Capital Medical University, Beijing, China (F.W.); Department of Neurosurgery, Beijing Tiantan Hospital, Capital Medical University, Beijing, China (F.W.); State Key Laboratory of Respiratory Health and Multimorbidity, Institute of Laboratory Animal Science, Chinese Academy of Medical Sciences & Peking Union Medical College, Beijing, China (X.P.)

References

1. Tan AC, Ashley DM, Lopez GY, Malinzak M, Friedman HS, Khasraw M. Management of glioblastoma: state of the art and future directions. *CA Cancer J Clin*. 2020;70:299-312. https://doi.org/10.3322/caac.21613
2. Stupp R, Mason WP, van den Bent MJ, et al. Radiotherapy plus concomitant and adjuvant temozolomide for glioblastoma. *New Engl J Med*. 2005;352:987-996. https://doi.org/10.1056/NEJMoa043330
3. Sarkaria JN, Kitange GJ, James CD, et al. Mechanisms of chemoresistance to alkylating agents in malignant glioma. *Clin Cancer Res*. 2008;14:2900-2908. https://doi.org/10.1158/1078-0432.CCR-07-1719
4. Lang F, Liu Y, Chou FJ, Yang C. Genotoxic therapy and resistance mechanism in gliomas. *Pharmacol Ther*. 2021;228:107922. https://doi.org/10.1016/j.pharmthera.2021.107922
5. Fletcher-Sananikone E, Kanji S, Tomimatsu N, et al. Elimination of radiation-induced senescence in the brain tumor microenvironment attenuates glioblastoma recurrence. *Cancer Res*. 2021;81:5935-5947. https://doi.org/10.1158/0008-5472.CAN-21-0752
6. Lowe SW, Cepero E, Evan G. Intrinsic tumour suppression. *Nature*. 2004;432:307-315. https://doi.org/10.1038/nature03098
7. Schmitt CA, Wang B, Demaria M. Senescence and cancer–role and therapeutic opportunities. *Nat Rev Clin Oncol*. 2022;19:619-636. https://doi.org/10.1038/s41571-022-00668-4
8. Kang TW, Yevsa T, Woller N, et al. Senescence surveillance of pre-malignant hepatocytes limits liver cancer development. *Nature*. 2011;479:547-551. https://doi.org/10.1038/nature10599
9. Tasdemir N, Banito A, Roe J, et al. BRD4 connects enhancer remodeling to senescence immune surveillance. *Cancer Discov*. 2016;6:612-629. https://doi.org/10.1158/2159-8290.CD-16-0217
10. Saleh T, Carpenter VJ, Bloukh S, Gewirtz DA. Targeting tumor cell senescence and polyploidy as potential therapeutic strategies. *Semin Cancer Biol*. 2022;81:37-47. https://doi.org/10.1016/j.semcancer.2020.12.010
11. Birch J, Gil J. Senescence and the SASP: many therapeutic avenues. *Genes Dev*. 2020;34:1565-1576. https://doi.org/10.1101/gad.343129.120
12. Salam R, Saliou A, Bielle F, et al. Cellular senescence in malignant cells promotes tumor progression in mouse and patient glioblastoma. *Nat Commun*. 2023;14:441. https://doi.org/10.1038/s41467-023-36124-9
13. Banasavadi-Siddegowda YK, Russell L, Frair E, et al. PRMT5-PTEN molecular pathway regulates senescence and self-renewal of primary glioblastoma neurosphere cells. *Oncogene*. 2017;36:263-274. https://doi.org/10.1038/onc.2016.199
14. Hu Y, Zhang M, Tian N, et al. The antibiotic clofoctol suppresses glioma stem cell proliferation by activating KLF13. *J Clin Invest*. 2019;129:3072-3085. https://doi.org/10.1172/JCI124979
15. Bailly C, Vergoten G. A new horizon for the old antibacterial drug clofoctol. *Drug Discov Today*. 2021;26:1302-1310. https://doi.org/10.1016/j.drudis.2021.02.004
16. Wang M, Shim JS, Li RJ, et al. Identification of an old antibiotic clofoctol as a novel activator of unfolded protein response pathways and an inhibitor of prostate cancer. *Br J Pharmacol*. 2014;171:4478-4489. https://doi.org/10.1111/bph.12800
17. Belouzard S, Machelart A, Sencio V, et al. Clofoctol inhibits SARS-CoV-2 replication and reduces lung pathology in mice. *PLoS Pathog*. 2022;18:e1010498. https://doi.org/10.1371/journal.ppat.1010498
18. Huang W, Hickson LJ, Eirin A, Kirkland JL, Lerman LO. Cellular senescence: the good, the bad and the unknown. *Nat Rev Nephrol*. 2022;18:611-627. https://doi.org/10.1038/s41581-022-00601-z
19. Milanovic M, Fan DNY, Belenki D, et al. Senescence-associated reprogramming promotes cancer stemness. *Nature*. 2018;553:96-100. https://doi.org/10.1038/nature25167
20. Patra S, Naik PP, Mahapatra KK, et al. Recent advancement of autophagy in polyploid giant cancer cells and its interconnection with senescence and stemness for therapeutic opportunities. *Cancer Lett*. 2024;590:216843. https://doi.org/10.1016/j.canlet.2024.216843
21. Wang Z, Zhang Y, Wu F, et al. Therapy-induced senescent glioblastoma cells sustain a procancer immune microenvironment by activating DDX58-mediated STAT1 signaling. *Neuro Oncol*. 2025;27:2265-2280. https://doi.org/10.1093/neuonc/noaf107
22. Jiang G, Tu J, Zhou L, et al. Single-cell transcriptomics reveal the heterogeneity and dynamic of cancer stem-like cells during breast tumor progression. *Cell Death Dis*. 2021;12:979. https://doi.org/10.1038/s41419-021-04261-y
23. Barakat R, Chatterjee J, Mu R, et al. Human single cell RNA-sequencing reveals a targetable CD8(+) exhausted T cell population that maintains mouse low-grade glioma growth. *Nat Commun*. 2024;15:10312. https://doi.org/10.1038/s41467-024-54569-4
24. Cancer GARN. Comprehensive genomic characterization defines human glioblastoma genes and core pathways. *Nature*. 2008;455:1061-1068.
25. Danesi R, Gasperini M, Senesi S, Freer G, Angeletti CA, Tacca D. M. A pharmacokinetic study of clofoctol in human plasma and lung tissue by using a microbiological assay. *Drugs Exp Clin Res*. 1988;14:39-43.
26. Newlands ES, Stevens MF, Wedge SR, Wheelhouse RT, Brock C. Temozolomide: a review of its discovery, chemical properties, pre-clinical development and clinical trials. *Cancer Treat Rev*. 1997;23:35-61. https://doi.org/10.1016/s0305-7372(97)90019-0
27. Stupp R, Gander M, Leyvraz S, Newlands E. Current and future developments in the use of temozolomide for the treatment of brain tumours. *Lancet Oncol*. 2001;2:552-560. https://doi.org/10.1016/S1470-2045(01)00489-2
28. Oliver L, Lalier L, Salaud C, Heymann D, Cartron PF, Vallette FM. Drug resistance in glioblastoma: are persisters the key to therapy? *Cancer Drug Resist*. 2020;3:287-301. https://doi.org/10.20517/cdr.2020.29
29. Lee SY. Temozolomide resistance in glioblastoma multiforme. *Genes Dis*. 2016;3:198-210. https://doi.org/10.1016/j.gendis.2016.04.007210
30. Joruiz SM, Von Muhlinen N, Horikawa I, Gilbert MR, Harris CC. Distinct functions of wild-type and R273H mutant Delta133p53alpha differentially regulate glioblastoma aggressiveness and therapy-induced senescence. *Cell Death Dis*. 2024;15:454. https://doi.org/10.1038/s41419-024-06769-5
31. Hirose Y, Berger MS, Pieper RO. p53 effects both the duration of G2/M arrest and the fate of temozolomide-treated human glioblastoma cells. *Cancer Res*. 2001;61:1957-1963.
32. Pawlowska E, Szczepanska J, Szatkowska M, Blasiak J. An interplay between senescence, apoptosis and autophagy in glioblastoma multiforme-role in pathogenesis and therapeutic perspective. *Int J Mol Sci*. 2018;19:889. https://doi.org/10.3390/ijms19030889
33. Chaib S, Tchkonia T, Kirkland JL. Cellular senescence and senolytics: the path to the clinic. *Nat Med*. 2022;28:1556-1568. https://doi.org/10.1038/s41591-022-01923-y
34. Tomimatsu N, Di Cristofaro L, Kanji S, et al. Targeting cIAP2 in a novel senolytic strategy prevents glioblastoma recurrence after radiotherapy. *EMBO Mol Med*. 2025;17:645-678. https://doi.org/10.1038/s44321-025-00201-x

35. Chang J, Wang Y, Shao L, et al. Clearance of senescent cells by ABT263 rejuvenates aged hematopoietic stem cells in mice. *Nat Med*. 2016;22:78-83. https://doi.org/10.1038/nm.4010
36. Tse C, Shoemaker AR, Adickes J, et al. ABT-263: a potent and orally bioavailable bcl-2 family inhibitor. *Cancer Res*. 2008;68:3421-3428. https://doi.org/10.1158/0008-5472.CAN-07-5836
37. Jiang X, Stockwell BR, Conrad M. Ferroptosis: mechanisms, biology and role in disease. *Nat Rev Mol Cell Biol*. 2021;22:266-282. https://doi.org/10.1038/s41580-020-00324-8
38. Yang WS, SriRamaratnam R, Welsch ME, et al. Regulation of ferroptotic cancer cell death by GPX4. *Cell*. 2014;156:317-331. https://doi.org/10.1016/j.cell.2013.12.010
39. Ursini F, Maiorino M, Gregolin C. The selenoenzyme phospholipid hydroperoxide glutathione peroxidase. *Biochim Biophys Acta*. 1985;839:62-70. https://doi.org/10.1016/0304-4165(85)90182-5
40. Hangauer MJ, Viswanathan VS, Ryan MJ, et al. Drug-tolerant persister cancer cells are vulnerable to GPX4 inhibition. *Nature*. 2017;551:247-250. https://doi.org/10.1038/nature24297
41. Tsoi J, Robert L, Paraiso K, et al. Multi-stage differentiation defines melanoma subtypes with differential vulnerability to Drug-Induced Iron-Dependent oxidative stress. *Cancer Cell*. 2018;33:890-904.e5. https://doi.org/10.1016/j.ccell.2018.03.017
42. Viswanathan VS, Ryan MJ, Dhruv HD, et al. Dependency of a therapy-resistant state of cancer cells on a lipid peroxidase pathway. *Nature*. 2017;547:453-457. https://doi.org/10.1038/nature23007
43. Ouyang S, Li H, Lou L, et al. Inhibition of STAT3-ferroptosis negative regulatory axis suppresses tumor growth and alleviates chemoresistance in gastric cancer. *Redox Biol*. 2022;52:102317. https://doi.org/10.1016/j.redox.2022.102317
44. Liu W, Chakraborty B, Safi R, Kazmin D, Chang CY, McDonnell DP. Dysregulated cholesterol homeostasis results in resistance to ferroptosis increasing tumorigenicity and metastasis in cancer. *Nat Commun*. 2021;12:5103. https://doi.org/10.1038/s41467-021-25354-4
45. Liu Y, Su Z, Tavana O, Gu W. Understanding the complexity of p53 in a new era of tumor suppression. *Cancer Cell*. 2024;42:946-967. https://doi.org/10.1016/j.ccell.2024.04.009
46. Gong L, Xu D, Ni K, et al. Smad1 promotes tumorigenicity and chemoresistance of glioblastoma by sequestering p300 from p53. *Adv Sci (Weinh)*. 2025;12:e2402258. https://doi.org/10.1002/advs.202402258
47. Wang YJ, Sun T, Xue ST, et al. A novel class of multi-substituted diaryl scaffold derivatives inhibit glioblastoma progression by targeting CD155. *Adv Sci*. 2025;12:e06688.